Structural Engineering and Mechanics, Vol. 26, No. 3 (2007) 343-361
DOI: http://dx.doi.org/10.12989/sem.2007.26.3.343

Numerical model for bolted T-stubs with two bolt rows

Alain Daidié[†]

Toulouse Mechanical Engineering Laboratory, INSA Toulouse, France

Jamel Chakhari[‡]

Toulouse Mechanical Engineering Laboratory, INSA Toulouse, France
Solid Mechanics, Structures and Technological Developments Laboratory, HSST Tunis, Tunisia

Ali Zghal[‡†]

Solid Mechanics, Structures and Technological Developments Laboratory, HSST Tunis, Tunisia

(Received June 12, 2006, Accepted December 4, 2006)

Abstract. This article presents a numerical tool for dimensioning two-threaded fasteners connecting prismatic parts subjected to fatigue tension loads that are coplanar with the screw axis. A simplified numerical model is developed from unidirectional finite elements, modeling the connected parts and screws with bent elements and the elastic contact layer between the parts with springs. An algorithm updating the contact stiffness matrix, calculating forces and displacements at each node of the structure and thus normal stresses in the screws in both static and fatigue is further developed using C language. An experimental study is also conducted in parallel with the numerical approach to validate the developed model assumptions, the numerical model and the 3D finite element results. Since stiffness values for the compressive zones in the parts are analytically difficult to determine, a statistical software method is used, from which a tuning factor is derived for identifying these stiffness values. The method is also applied to set out the influence of each parameter on the fatigue behaviour of each screw. Finally, the developed model will be used to establish a new, sophisticated, fast and accurate tool for dimensioning bolted mechanical structures.

Keywords: bolted connections; numerical modeling; finite elements; structures.

1. Introduction

Bolted joints, easy and quick to manufacture and implement, are used for assembling the majority of mechanical subassemblies in mechanical, civil, and aeronautical constructions. Hence they are often subjected to static or cyclic dynamic loads that may lead to fatigue failure. This is why manufacturers always seek new sophisticated and quick dimensioning tools and softwares that can

† Associate Professor, Corresponding author, E-mail: alain.daidie@insa-toulouse.fr
‡ Ph.D., Research Assistant, E-mail: ch_jamel@yahoo.ca
‡† Professor, E-mail: ali.zghal@esstt.rnu.tn

replace the conventional calculation methods.

Within this framework, several researchers working on preloaded T-stub connections use non linear finite elements modeling like in Bursi and Jaspart (1997a), Sherbourne and Bahaari (1997), Kishi *et al.* (2001), Komuro *et al.* (2004). These studies specifically deal with steel structures and are interested in the behaviour of the structure in displacement. Bursi and Japart (1997b) showed a good correlation between numerical 3D simulations and experimental tests, while Girao *et al.* (2004) replaced the bolt with a set of parallel uniaxial spring elements. In the context of a load-displacement analysis, these models accurately retrieve the behaviour of the structure without studying the fatigue strength, the local behaviour of the bolts and their resistance when subjected to dynamic solicitations.

The bent beam model is a base point for many developments while the most frequently used model is the one proposed by the VDI 2230 (2003) recommendation. It is, unfortunately limited to bolted joints with axial or weakly eccentric loading since for high eccentric loading and thus high bending, the hypothesis of non detachment between connected parts at contact interface is no longer accurate. Agatonovic (1985) established a model that takes into account the two main parameters: bending stiffness of the connected parts and preloading value.

From these recent studies, a model for heavy eccentric loaded connections is developed at the Toulouse Mechanical Engineering Laboratory. Guillot (1987) improved the Agatonovic model by introducing a parameter that depends on load application position. Bakhiet (1994) established an analytical formulation that takes into account the largeness of the contact zones, while Bulatovic and Jovanovic (2000) developed an analytical model for an eccentrically loaded bolted joint and outlined the deformation of the contact zone under loading. Note that all the previously described models are related to a single-bolted fastener subjected to a load parallel to the bolt axis and use linear springs for modeling the compressed zone and the bolt's traction stiffness. They can be applied in the framework of dimensioning a symmetrical bolted T-joint frequently used in metallic structures studied by Broughton *et al.* (2004).

Throughout the modeling process, difficulties are basically encountered in formulating joints compression and bending stiffness of the parts. The VDI 2230 (2003) recommendation, which considers a cone deformation zone having the same stiffness as the real zone (Lehnhoff *et al.* 1994), entails a purely geometrical approach to cover the stacking of parts with different heights. Allen (2003) and Alkatan (2005) applied the energy method to set out the stiffness of the bolts under traction and the parts under compression, Tsai and Kelly (2005) formulated the lateral stiffness of a short beam loaded at its edge, while Zaharia and Dubina (2006) developed the rotational stiffness of four or six-bolted connections.

Many research studies have been devoted to dimensioning multi-bolted connections. In this area, Al-Jabri *et al.* (2006) modeled a beam-column connection assembled by three or six bolts subjected to an external moment and at high temperature.

A non-linear model or bent beam model has been developed at the mechanical engineering laboratory of Toulouse (LGMT), Guillot (1987), that can be applied to rectangular and circular joints. Marty (1994) modeled a circular flanged connection as a bent plate laying on its lower compressed part, subdivided into the same stiffness linear springs elements. A finite element program is also established upon a model based on axis-symmetrical plate elements for forces and bending moment calculation.

Kowalske (1973) represented the beam resting on its lower half by a limited number of springs. A subsequent development of this model can be found in Oden and Pires (1983) studies in which a

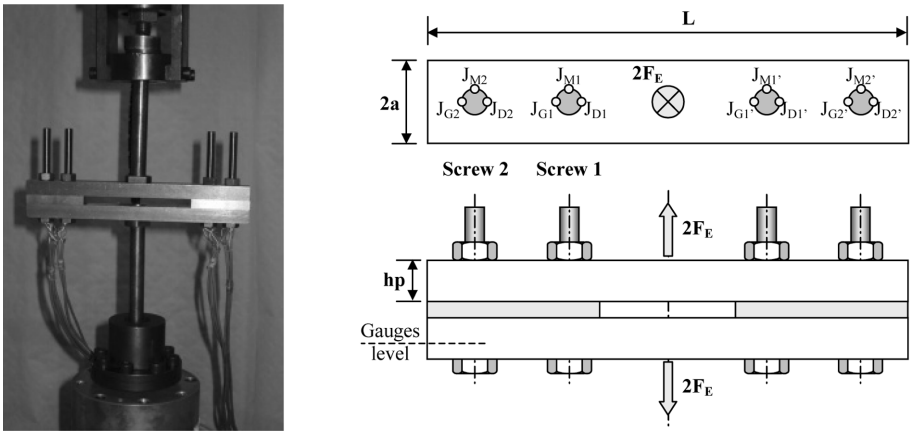

Fig. 1 Experimental study of a symmetrical four bolted connection subjected to tensile loading

model based on bent beams fixed by one or more bolts is developed. In this approach, loads are introduced as single forces, moments and distributed forces and the beam's displacement is analytically calculated through an iterative process. Throughout every iteration, the node penetration displacement in the elastic layer is calculated. The vertical displacement sign of each contact node is verified in the next iteration.

Unfortunately, all the available models are limited to only well-defined and simple geometrical connections. since they are not always able to specify the various contact areas (adherence, contact separation, slippage, etc.). Even models that include elastic contact layers do not pinpoint the determination of the contact evolution and the elements stiffness under external loading.

This article presents a model for dimensioning two-threaded fasteners connecting prismatic parts subjected to fatigue tension loads that are coplanar with the screw axis. Its application is not limited only to the field of general mechanics and structures with thick parts, but also to structures with thin parts as in the field of constructional steelwork.

A sophisticated model which can be described as a "simplified numerical model" is developed : it simulates contact by a series of springs whose number changes with loading. Experimental studies are required to verify the results of this model and the adopted hypothesis (Fig. 1). This experimental work analysed the real behaviour of the studied connection and allowed the simplified numerical model to be well tuned. Three comparative studies validated the general behaviour of the model. Moreover, it is not limited to standard problems as shown in Fig. 1, and it can be extended to dimensioning multi-threaded connections submitted to eccentric loading.

2. Simplified numerical model

2.1 Model presentation

A prismatic connection with two identical screws is considered. The subassemblies are fixed to a rigid support (Fig. 2a) and have a rectangular cross-section ($2a \times h_p$). Bending stiffness and compression stiffness are considered constant with loading and the load axis is coplanar with the screw axis. Since the bending stiffness of the parts is more significant than the stiffness of the

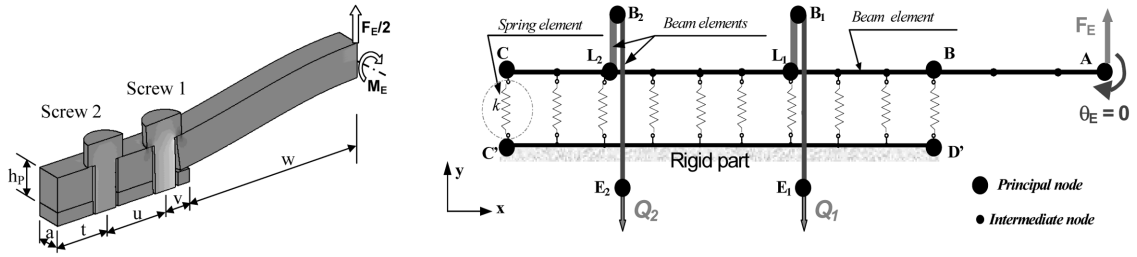

a : 3D-Finite Elements model b : Simplified numerical model

Fig. 2 Two bolted symmetrical connections subjected to tensile loading. Screw axis and load are on the same plane

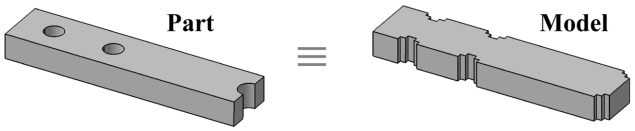

Fig. 3 Holes are modeled in successive elements

screws, the bending moment applied at the screw heads on the connected parts can be discarded and the screws are respectively preloaded by nodal forces Q_1 and Q_2.

The one-dimensional finite elements model shown in Fig. 2(b) represents the structure subjected to a vertical positive load F_E, a moment M_E. A null rotation θ_E around the z axis is applied at extremity A to accurately represent the symmetry of the experimental connection (Fig. 1).

The numerical model consists of the following elements:

Beam elements (part CA) **:** The bending stiffness of these bi-nodal elements is equal to the real stiffness of the prismatic part. The hole is modeled by a succession of beam elements whose width varies progressively with scale form (Fig. 3) to simulate the stress concentration that occurs in the holes of the real bolt. The real part and the model are equivalent in bending stiffness and strain. Note that in the numerical simplified model, half of the part is considered. The numerical model is developed to predict bolts stresses. It should also be noted that a traction and bending stress concentration factors must be taken into account when calculating the stresses in the subassemblies to take into consideration the holes effects.

Beam elements B_1L_1 and B_2L_2: B_1L_1 and B_2L_2 represent the portion of the subassemblies located between the load application level and the screw heads considered as two beam elements with equivalent cross-sections A_P calculated using one of the following existing models: VDI 2230 (2003), Rasmussen model (Rasmussen *et al.* 1978) and the LGMT model (Alkatan *et al.* 2003). The two nodes of each beam are kinematically coupled in rotation around the z axis since it is considered that the screw heads follow the part deformation.

Beam elements (bolts B_1E_1 and B_2E_2)**:** Each bolt is modeled with a bi-nodal super-beam element that has a special stiffness matrix with three degrees of freedom at each node: u, v and θ (axial displacement, transverse displacement and rotation). Partitioning is unnecessary since displacements at the extremities (boundaries) are used to calculate axial load F_B and bending moment MF_B for each section and thus, normal stresses along the screws. The stiffness matrix includes the real axial stiffness of the screw taking into account an equivalent section A_{bi} whereas the bending stiffness is

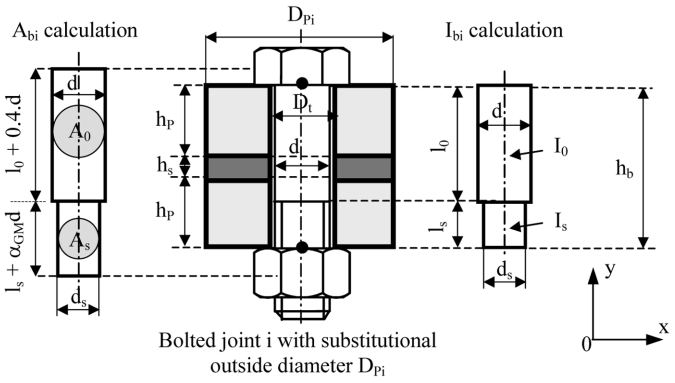

Fig. 4 Equivalent section and equivalent inertia moment of bolts

calculated using an equivalent inertia moment I_{bi} that includes the screw shape (Fig. 4).

Thus, the problem consists of establishing the stiffness matrix of an equivalent beam with the following properties: length h_b equal to grip, circular section A_{bi}, bolt modulus of elasticity E_b and the same stiffness characteristics as the real bolt. The compression stiffness calculation procedure includes the tapping ($a_{GM} = 0.8$) or bolt head and screw influence ($a_{GM} = 1$) (VDI 2230 2003, Fukuoka 1994, Alkatan 2005). The Equivalent section A_{bi} is calculated using the following expression

$$A_{bi} = \frac{h_b}{\frac{l_0 + 0.4d}{A_0} + \frac{l_s + \alpha_{GM}d}{A_s}} \tag{1}$$

Note that Eq. (1) is derived from the relation below

$$\delta_{Bi} = \frac{1}{E_b}\left[\frac{l_0 + 0.4d}{A_0} + \frac{l_s + \alpha_{GM}d}{A_s}\right] \equiv \frac{h_b}{E_b A_{bi}} \tag{2}$$

The equivalent quadratic moment, given by I_{bi} Eq. (4) is calculated from the equivalent bending stiffness Eq. (3), which can be obtained by summing the bending stiffness of cylindrical portions

$$\delta_{FBi} = \frac{1}{E_b}\left[\frac{l_0}{I_0} + \frac{l_s}{I_s}\right] \equiv \frac{h_b}{E_b I_{bi}} \tag{3}$$

$$I_{bi} = \frac{h_b I_0 I_s}{l_0 I_s + l_s I_0} \tag{4}$$

$$h_b = 2h_P + h_s \tag{5}$$

It should be noted that only a rotation movement is imposed at the bolt extreme sections, whereas radial displacements are negligible and displacement is free inside the hole. Screws are subjected to pure bending and displacement is set free along the x axis at points E_1 and E_2 (Fig. 2b) to minimize error due to the position of the section where results are extracted and for model tuning up. The moment applied on bolt i (Fig. 2), is given by the following equation

$$MF_{Bi} = \frac{2E_b I_{bi}}{h_b}\theta_{Bi} \tag{6}$$

where θ_{Bi} represents the rotation of head B_i of bolt i (i = 1 or 2). Since the sub assemblies are fixed with screws to a rigid part, nodes E_1 and E_2 are blocked. The bending moment is not constant along the screw and can be expressed using the beam deformation equation

$$E_b I_{bi} v'' = MF_{Bi} \tag{7}$$

The initial stresses are respectively σ_{01} and σ_{02}, whereas Q_1 and Q_2 are the respective preloads applied to screws 1 and 2. Therefore, displacements u_{01} and u_{02} are respectively applied to the lower bottoms E_1 and E_2 of the screws for preload modeling. Subsequently, axial loads F_{B1} and F_{B2}, bending moments MF_{B1} and MF_{B2}, necessary for fatigue dimensioning can be calculated. Load variation (ΔF_{Bi}) and bending moment variation (ΔMF_{Bi}) between the preloaded state and the loading state can be calculated for bolt i, using the following two equations

$$\Delta F_{Bi} = F_{Bi} - Q_i \tag{8}$$

$$\Delta MF_{Bi} = MF_{Bi}(F_E) - MF_{Bi}(Q_i) \tag{9}$$

As a result, alternate stress (σ_{ai}) on each bolt can be calculated by Junker (1986)

$$\sigma_{ai} = \frac{\Delta F_{Bi}}{2 \cdot As_i} + \frac{\Delta MF_{Bi} \cdot ds_i}{4 \cdot I_{b_i}} \leq \sigma_D \tag{10}$$

where ds_i is the diameter of the screw cross-section As_i having a quadratic moment I_{bi}, and σ_D is the European standard (E25-030 1988) material alternating stress limit of the screws.

At loading phase each bolt is subjected to normal and tangential stresses given by the following relations

$$\sigma = \frac{F_{Bi}}{A_s} + \frac{32MF_{Bi}}{\pi d_{si}^3} \tag{11}$$

$$\tau = \frac{16C_b}{\pi d_{si}^3} \tag{12}$$

Thus, Von Mises criteria are applied for static dimensioning, using the 2 expressions below

$$\sigma_{eq} = \sqrt{\sigma^2 + 3 \cdot \tau^2} \tag{13}$$

$$\sigma_{eq.\max} \leq S_y \tag{14}$$

where S_y is the yield strength of the bolt class quality and C_b the tightening torque.

The dynamic behaviour of a standard bolt (thread rolling screw with final heat treatment) is practically independent from the class quality. Moreover, the dynamic resistance is a little influenced by the static loading generated by to the mean stress state (σ_m = 0.5 to 0.8S_y of the class quality) (Martinez-Martinez 2002, VDI 2230 2003, E25-030 1988, Fares *et al.* 2006a). Experimental

fatigue tests on a bolted joints must be comply with the norm NF E27-009 (1979). Fares (2006b) and VDI 2230 (2003) noted that 85% of failures take place at the first engaged thread. This may be due to high local stress concentrations combined with load distribution between screw and bolt. The screw resistance under alternating solicitations is low compared to a static loading case. Norm E25-030 (1979) and VDI 2230 (2003) take into account stress concentration at the thread bottom, and thus recommend values for the fatigue limit of high-strength bolts at the stress cross-section A_s proceeding from Wöhler curves, following an uniaxial fatigue approach. The fatigue solicitation is the normal stress variation between preloading and loading phases at the screw cross section, resulting from traction loading and bending moment variation. The T-Stub flanges field is considered a high cycle fatigue sector, since $N_D \geq 2.10^6$ cycles. For a mounting using M10 8.8 screws, the endurance limit should not exceed σ_D = 50 MPa.

Blocked nodes (part C'D') : Segment C'D' made up of rigid elements, represents the part's base support.

Spring elements : These linear elastic elements are inserted along the contact zone to simulate contact between subassemblies. Their number is function of the interface detachment, depending on external tensile loading, and stiffness distribution is proportional to the theoretical area. These springs are associated with friction elements to take into account the adherence zone. Normal stress at the contact interface is calculated from the relative vertical displacement between the interface contact nodes and the neutral line nodes of part (CA), using the following relation

$$\sigma_n = k_i \cdot u_n \tag{15}$$

Hence, the tangential stress is set out using Coulomb's friction law given by

$$\sigma_t = f \cdot \sigma_n \tag{16}$$

where u_n is the relative normal displacement of spring nodes, σ_n and σ_t respectively the normal and tangential stresses at the contact interface depending on the spring position. f is the friction coefficient at the contact interface.

The spring i stiffness k_i is calculated using the following expressions

$$K_T = \sum_{i=1}^{N} k_i;\ k_i = \frac{S_i}{S} K_T;\ S_i = \frac{\left|X_{i-1} - X_{i+1}\right|}{2} \cdot 2a \tag{17}$$

where N is the total number of spring elements, S the total contact area surface, S_i the contact area surface modeled by spring i and located at abscissa X_i, and K_T the total stiffness of elastic layer modeling the parts contact.

Equivalent diameter D_P of the compressed zone located between the screw-heads and the rigid part, calculated by the Rasmussen method, is used to determine compression stiffness K_{pi} of the zone located between screw i head and the rigid part. $K_{p\,eq}$ defined as the equivalent compression stiffness of zones located between screw heads and the rigid part is calculated using the following expression

$$K_{p\,eq} = K_{p1} + K_{p2} \tag{18}$$

REP is the stiffness distribution factor defined in the equation below

$$REP = \frac{K_T}{K_{p\,eq}} \tag{19}$$

This factor is equal to the stiffness ratio between the elastic layer located between the middle line of the connected part and the rigid body, and the equivalent stiffness of the two compressed zones under the screw heads. A value of 0.75 for this factor is found in experimental tests similar to the ones conducted by Vadean (2006).

2.2 Numerical resolution

The numerical resolution is supported by an iterative numerical method. At each iteration, the contact zone is re-defined and a finite dimensional system of linear equations resolved. Nodal displacements are calculated using the numerical contact identification presented in Algorithm 1 into which a tightening condition is injected at the lower base of each screw.

$$\left[\begin{array}{l} \text{While} \quad \dfrac{\left\| \delta^n - \delta^{n-1} \right\|}{\left\| \delta^n \right\|} \geq eps \\ \text{Solve} \quad ([R_g] + [R_c^{n-1}])\{\delta^n\} = \{F\} \\ n-1 \leftarrow n \end{array}\right.$$

Algorithm 1 Numerical identification of node displacements and contact stiffness matrix knowing boundary conditions and force vector

In this algorithm, $\| \delta^n \|$ represents the Euclidean norm of the generalised displacement vector $\{\delta^n\}$, composed of nodes displacements of the meshed structure at iteration n. Stiffness matrix $[R_g]$ is assembled from the elementary stiffness matrices of all beam elements of the model. Contact stiffness matrix $[R_c^{n-1}]$ of the elastic layer is established by assembling the elementary stiffness matrices of active springs at iteration $(n-1)$. A spring i can be considered active or not after verification of the sign of its relative displacement (δ_i^{n-1}). Stiffness matrices of model elements are expressed in the Appendix (Razavi 2004, Rockey *et al.* 1983).

2.3 Calculation steps

A program which defines nodes coordinates and elements properties was developed in C language. Subsequently, it calculates stiffness matrices of various elements. The overall stiffness matrix of the structure is calculated by bringing $[R_g]$ and $[R_c]$ matrices. Force variation $\Delta F_{Bi}(Q_i)$ and bending moment variation $\Delta MF_{Bi}(Q_i)$, in threaded fasteners are calculated in two steps as shown in Algorithm 2.

At preload phase, displacements at the lower ends of each screw, force variations ($\Delta F_{Bi}(Q_i)$) and bending moment variations ($\Delta MF_{Bi}(Q_i)$) on each screw, are calculated.

At loading phase, displacements at the two lower ends of the screws (nodes E_1 and E_2), found in the previous step are applied. After iterative calculation, force variations and moment variations, stresses and alternating stresses on bolts are deduced and safety is verified under static and fatigue conditions.

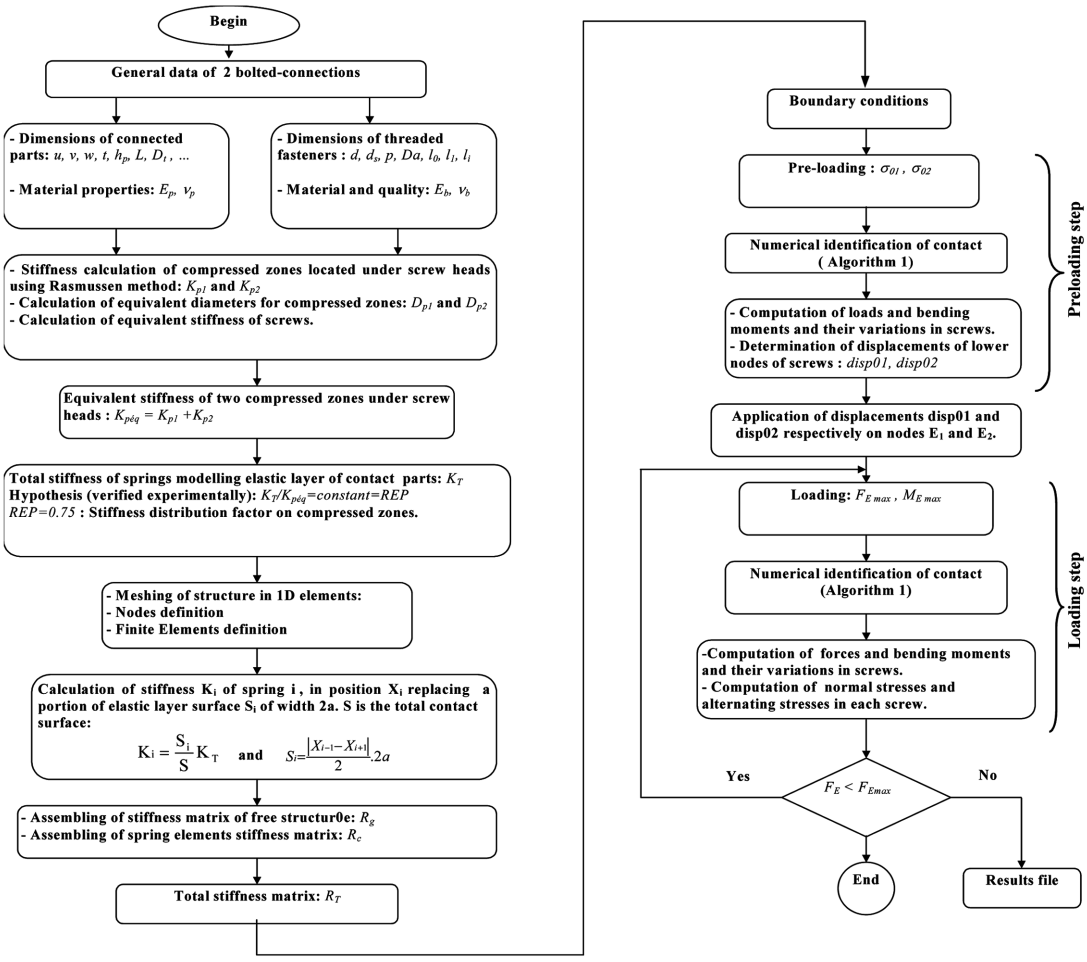

Algorithm 2 Calculation steps for T-stub model resolution

3. Experimental tests

The experimental set-up is a symmetrical connection sample of four identical H M10-60 8.8 quality screws, subjected to a monotonic tensile loading generated by a 100 kN capacity hydraulic machine. Each screw is equipped, along its reduced length, with three deformation gauges set at 90° to verify the load symmetry of the experimental connection. These gauges are linked to an electronic box and data acquisition software.

The experimental design method guides the number of tests and tube dimensions choice. Even so, this technique could not be considered as a more recent Fischer technique (1926), nor could it be systematically used in the industrial, agronomic, medical and mechanical sectors (Kuehl 1999, Montgomery 2000, Daidié *et al.* 2002, Gitlow *et al.* 2006) before the publication of Taguchi's works (1978, 1987, 2001). Its main contribution lies in minimizing the number of tests, while allowing better results interpretation. In an experimental design method, several factors are modified from one experiment to another according to precise rules. Consequently, parameters sensitivity can

be investigated with the objective of seeking better result accuracy.

Finally, a study was conducted on 18 experimental mounting cases (Tables 1, 2 and 3), where the geometrical parameters are varied along 3 levels (h_p, a, L, u and v) and 2 levels according to the material: steel and aluminium, whereas the base thickness h_s remained constant (h_s = 10 mm). Note that a complete plan requires $3^5 \times 2^2 = 972$ tests and a statistical software that includes pre-formulated tables. JMP (2005) commercial software was used in this study and a mixed factorial plan is chosen to reduce the number of experiments to 18 and to draw conclusions about the influence of several parameters on screw's behaviour under fatigue.

4. Experimental validation of numerical models

The previously presented model is developed using the REP coefficient. This coefficient is important to reproduce the real joint behaviour and to show good correlation between the experimental results, 3D Finite Elements calculations and the developed model.

3D Finite elements calculations are carried out with I-DEAS 11 NX (2004) software. Note that the 3D model represents 1/8 of the experimental assembly (Fig. 5) and the displacement boundary conditions are defined at the three symmetry planes. The subassemblies are meshed with solid linear brick elements. Preloads are introduced as imposed uniaxial displacements δ_{0i} at the bottoms of the screws. Thus, a two steps simulation procedure is necessary to respectively install the preloads and vary the external loading. The friction coefficient at the contact interfaces is equal to 0.14. The F_E equivalent load is applied on the vertical common edge of the symmetry planes.

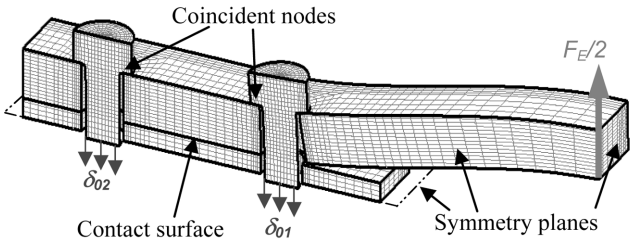

Fig. 5 3D finite elements model for a T-stub study

Table 1 Numerical data for three connection examples

Data	Connection 1	Connection 2	Connection 3
h_p (mm)	13	20	20
$2a$ (mm)	30	40	40
L (mm)	290	250	250
u (mm)	45	25	25
v (mm)	25	25	25
Part material	C 35 E	C 35 E	Al Cu 4 Mg Si (A)
Measured preloads on screw 1 : σ_{01} (MPa)	206.379	207.878 MPa	203.786
Measured preloads on screw 2 : σ_{02} (MPa)	210.116	207.204 MPa	204.627
REP	0.75	0.75	0.75

The results of three examples of experimental connections are presented. Numerical data for the different connections are given in Table 1 and results are compared (Figs. 6, 7 and 8) for an objective pre-stress of 200 MPa. For each loading increment, alternating stress is calculated using Eq. (10). By numerical simulations, screw stresses can be computed above their real capacities to predict screw behaviour under heavy loads. Note that the screws maximum fatigue capacities are experimentally reached and evaluated as an effective alternating stress limit of 60 MPa (Fares 2006a).

Conformability between the simplified numerical model, 3D finite element simulations and experimental results is necessary to identify the REP factor.

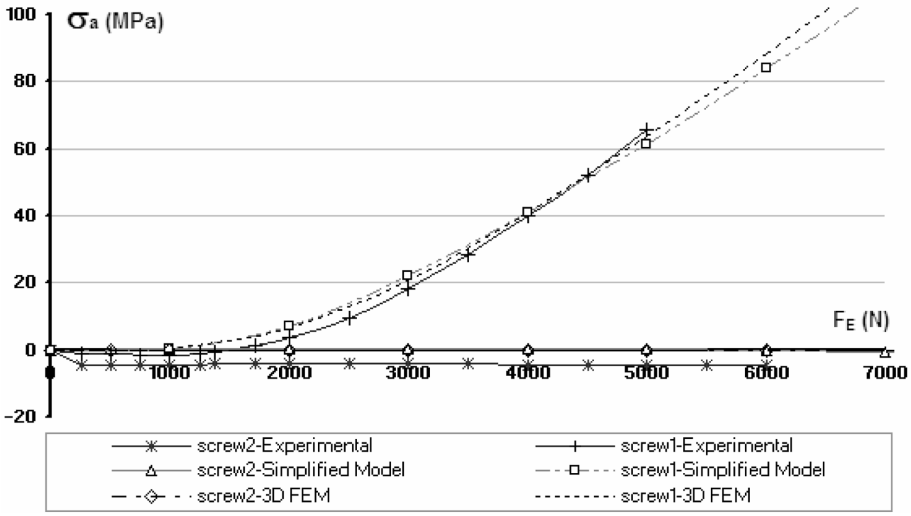

Fig. 6 Comparison of results, $0 \le F_E \le F_{E\max}$ for connection 1

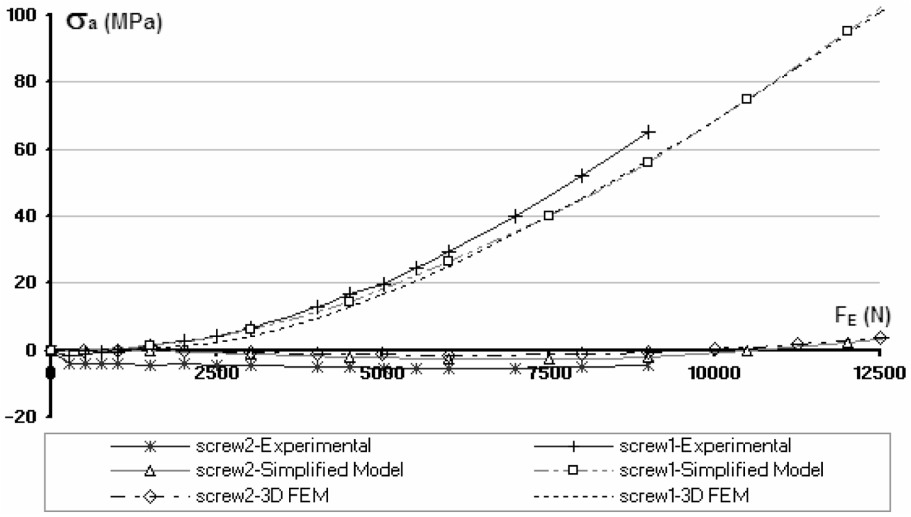

Fig. 7 Comparison of results, $0 \le F_E \le F_{E\max}$ for connection 2

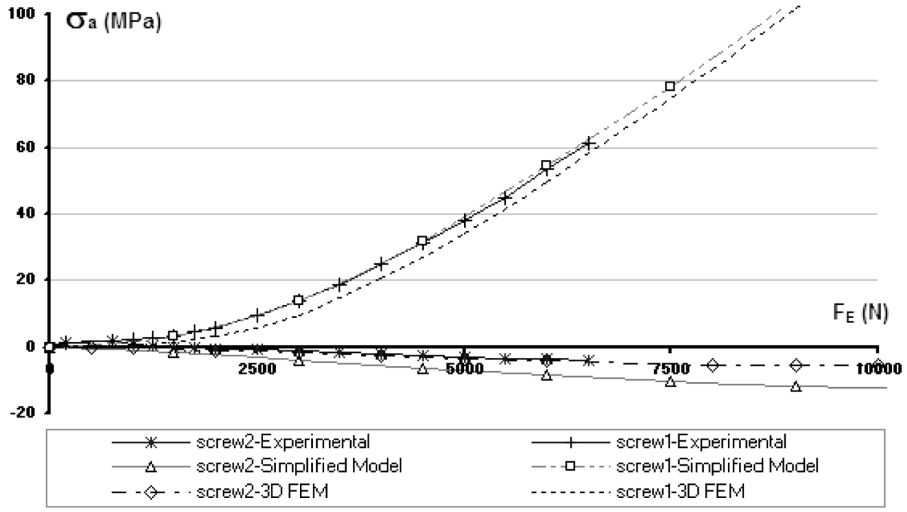

Fig. 8 Comparison of results, $0 \leq F_E \leq F_{E\max}$ for connection 3

For connection 1 (Fig. 6), the experimental and numerical curves match. However, Screw 2 is subjected to negative light alternating stresses, thus contributing to connection stability. Fatigue dimensioning must be relative to screw 1 since the admissible conventional fatigue stress of 50 MPa (E25-030 1988) for H M10-60, 8.8 quality screws is reached under an external loading of 4500 N.

The experimental curves and numerical models also match for connection 2, (Fig. 7). However, screw 2, loaded to 10000 N stabilises the connection. Note that the considerable alternating stresses along this screw are due to the dimensions of the subassemblies cross-section ($h_p = 20$ and $2a = 40$ mm).

Fig. 8 shows the results relative to an aluminium connection similar to connection 2. Investigating connection 3 shows that experimental tests, 3D calculation and simplified numerical model results match, thus showing similar behaviour.

Finally, stiffness distribution factor *REP* has the same 0.75 value in the three examples. An experimental design method is then used to validate this value and set out the effect of each joint parameter on the screws behaviour.

5. Effect of the various parameters on screw stresses

Bolts stresses at a given external loading, depend on different joint parameters (preload, material elasticity, joint dimensions).

5.1 Preload effect

Two different preload values are applied to joint 2: $\sigma_{01} = \sigma_{02} = 200$ MPa and 300 MPa. From the results presented in Fig. 9, one can conclude that fatigue stresses decrease with increasing preloads on screws.

5.2 Material and geometrical effects

A statistical method is applied to analyse the effects of various parameters (E_p, u, v, b, h_P) on the screws alternating stresses. Hence a combined experimental design with five factors and various levels is established and the statistical method is underpinned by a mixed 18 values factorial pattern covering 5 factors (Table 2) with 2 outputs:

Output 1 : Alternating stress on screw 1 : σ_{a1}

Output 2 : Alternating stress on screw 2 : σ_{a2}

The parameters with the most influence are chosen, and load eccentricity distance w (Fig. 2a) is not taken into account since it mostly influences the connected part in bending. Thus varying v is sufficient.

Table 2 Factors and levels with mixed experimental plan

Factors	Description	Level 1	Level 2	Level 3
A (MPa)	E_p	74000	21000	--------
B (mm)	u	25	35	45
C (mm)	v	10	20	25
D (mm)	b (= $2a$)	20	30	40
E (mm)	h_P	13	16	20

Table 3 Alternating stresses on screws 1 and 2 for 18 cases of the combined experimental plan, where σ_{01} = σ_{02} = 200 MPa and F_E = 4500 N

Case N°	E_p (MPa)	u (mm)	v (mm)	b (mm)	h_p (mm)	Screw 1 σ_{a1} (MPa)	Screw 2 σ_{a2} (MPa)
1	74000	25	10	20	13	142.63	–8.66
2	74000	25	20	30	16	71.78	–8.58
3	74000	25	25	40	20	31.87	–6.55
4	74000	35	10	30	20	46.53	–4.88
5	74000	35	20	40	13	78.88	–3.51
6	74000	35	25	20	16	92.67	–3.42
7	74000	45	10	40	16	53.73	–0.18
8	74000	45	20	20	20	57.27	–2.29
9	74000	45	25	30	13	94.63	0.20
10	210000	25	10	20	13	94.69	–6.44
11	210000	25	20	30	16	35.89	–4.76
12	210000	25	25	40	20	14.49	–2.00
13	210000	35	10	30	20	22.01	–2.77
14	210000	35	20	40	13	40.34	–1.72
15	210000	35	25	20	16	48.53	–3.14
16	210000	45	10	40	16	27.21	–1.20
17	210000	45	20	20	20	29.44	–2.18
18	210000	45	25	30	13	50.64	–0.42

Alternating stress values are extracted from the simplified numerical model with a stiffness distribution factor *REP* equal to 0.75. The results presented in Table 3 are compared to 3D numerical simulations and experimental results and the coherence between results is verified.

For each factor, a variance analysis of 5% risk in the ultimate case is conducted to identify the most determining factors. Moreover, the residual normality test is performed for each output to verify the normal distribution of estimator coefficients and the effect each factor has on screw alternating stresses is set out using JMP (2005) statistical software.

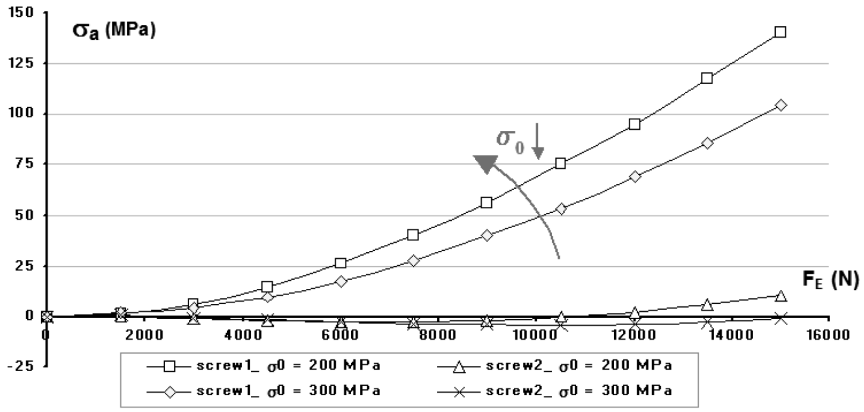

Fig. 9 Comparison of results for two different preloading tests on connection 2

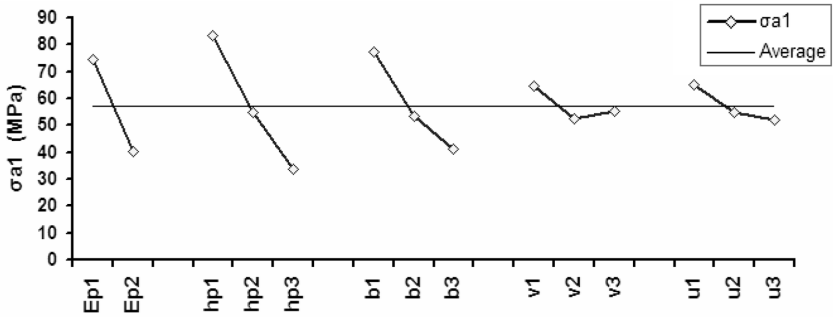

Fig. 10 Effects of Young modulus and geometrical parameters on alternating stresses of screw 1

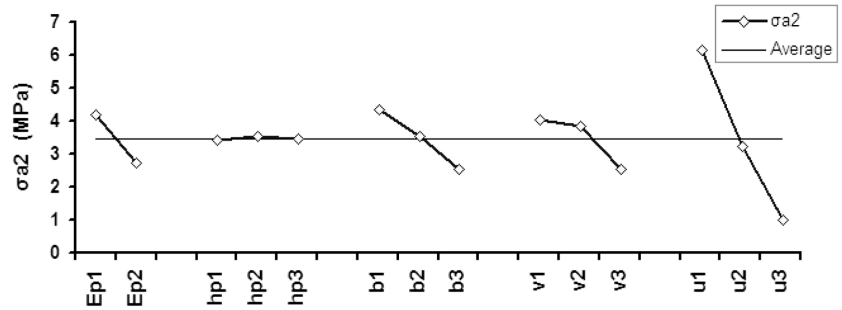

Fig. 11 Effects of Young modulus and geometrical parameters on alternating stresses on screw 2

5.2.1 Subassemblies Young modulus effect

The subassemblies are made of steel (C 35 E) or aluminium (Al Cu 4 Mg Si (A)), whereas the bolts are of steel only. The effect of E_P on screw alternating stresses is shown in Figs. 10 and 11. One can conclude that the absolute values of alternating stresses decrease with the Young modulus increase. This can be explained physically by bending in the subassemblies, and the screws bending decreases when its material is more rigid.

5.2.2 Effects of geometrical parameters on screw 1 alternating stresses

Fig. 10 shows the effect of each geometrical parameter on screw 1 alternating stresses. For fixed preload and external loading, alternating stress (σ_{a1}) on screw 1 decreases as u, b and h_p increase whereas it is slightly influenced by parameters u and v. σ_{a1} highly depends on the subassemblies section dimensions b and h_p. These parameters are directly related to the quadratic moment and part bending.

5.2.3 Effect of geometrical parameters on screw 2 alternating stresses

Fig. 11 shows the effect of each geometrical parameter on screw 2. For fixed preload and external loading, alternating stress (σ_{a2}) slightly varies with v, b and h_p. The main influencing parameter is screw axis distance u, since the absolute value of σ_{a2} decreases when u increases. In conclusion, alternating stresses decrease when the preload increases. Furthermore, fatigue stresses decrease when subassembly cross-section dimensions and material rigidity increase. Finally, alternating stresses on screw 2 are more significant when two screws are closer to each other.

6. Conclusions

In this paper, a developed numerical model for dimensioning two-threaded fasteners connections, and computing the displacements and forces at each node of the structure is presented. The model locates the contact zone, identifies the limit of interface separation for any compressive loading and calculates screws stresses for static or dynamic dimensioning.

Experimental and numerical results showed that the second screw, the least subjected to bending, increases loaded connection adherence, contributes in the assembly stiffness and decreases the alternating stress on screw one. In various configurations alternating stress limit (σ_D) is first reached on screw one.

Coherence between the experimental and numerical results validated the performance of the model. A large number of different configurations are investigated using an experimental method and a statistical software to show the effects of various factors on the screws alternating stresses.

The coded model has the advantage of rapidly computing these connections compared to 3D finite elements calculations. A similar model for dimensioning connections subjected to compressive loading is actually being developed. In this case an additional problem is encountered in the modeling of the contact between subassemblies and the angle corner of a rigid part, and calculating the stiffness of that contact zone. Additional experimental results will be conducted to study the influence of geometrical and materials parameters. This work will be the subject of a future publication.

References

Agatonovic, P. (1985), "Beam model of bolted flanged connection", *En. Comput.*, March 21, **2**, Pineridge Press Ltd, 21-29.

Al-Jabri, K.S., Seibi, A. and Karrech, A. (2006), "Modelling of unstiffened flush end-plate bolted connections in fire", *J. Constr. Steel Res.*, **62**, 151-159.

Alkatan, F., Stephan, P. and Guillot, J. (2003), "Equivalent stiffness of screw head in preloaded bolted connections", *Proc. of 8th AIP-PRIMECA National Congress*, March, La Plagne-Montalbert France, 1-10.

Alkatan, F. (2005), *Stiffness Modeling of Preloaded Threaded Elements Connections*. PhD Thesis, INSA of Toulouse France, Order N° 809, December.

Allen, C.T. (2003), *Computation of Bolted Joint Stiffness Using Train Energy*. Thesis, UMI 1417397, Huntsville, Alabama.

Bakhiet, E. (1994), *Study of Bolted Connections Strongly Eccentric Loaded and Subjected to Fatigue Stresses*, PhD Thesis N° 319, INSA of Toulouse France.

Broughton, W.R., Cracher, L.E., Grower, M.R.L. and Shaw, R.M. (2004), *Assessment of Predictive Analysis for Bonded and Bolted T-Joints*, Project MMS11, Report 4.

Bulatovic, R. and Jovanovic, J. (2000), "An analysis of the mathematical models in deformation process of eccentrically loaded bolts", *Mech. Eng.*, **1**(7), 789-797.

Bursi, O.S. and Jaspart, J.P. (1997a), "Benchmarks for finite element modelling of bolted steel connections", *J. Constr. Steel Res.*, **43**(3), 17-42.

Bursi, O.S. and Jaspart, J.P. (1997b), "Calibration of a finite element model for isolated bolted end-plate steel connections", *J. Constr. Steel Res.*, **44**(3), 225-262.

Daidié, A., Lakiss, H., Leray, D. and Guillot, J. (2002), "Application of the design of experiments method to a transversely loaded cylindrical assembly", *Integrated Design and Manufacturing in Mechanical Engineering*, KLUWER Academic Publishers, ISBN 1-4020-0979-8, 423-430.

Europan Standard E25-030 (1988), *Fasterners. Threaded Connections. Design, Calculation and Mounting Conditions*, AFNOR Publications, 2nd version, February, ISSN 0335-3931.

Fares, Y., Chaussumier, M., Daidié, A. and Guillot, J. (2006a), "Determining the life cycle of bolts using a local approach and the Dang Van criterion", *Fatigue Fract. Eng. M.*, **29**(8), 588-596.

Fares, Y. (2006b), *Fatigue Dimensioning of Bolted Assemblies Using Multiaxial Fatigue Criterion*, PhD Thesis, N° 847, INSA of Toulouse France.

Fischer, R.A. (1926), "The arrangement of field experiments", *J. the Ministry of Agriculture of Great Britain*, Scotland, 503-513.

Fukuoka, T. (1994), "Analysis of the tightening process of bolted joint with a tensioner using springs elements", *J. Pressure Vessel Technol.*, ASME, **116**, 443-448.

Girão Coelho, A.M., Simões da Silva, L. and Bijlaard, F.S.K. (2004), "Characterization of the nonlinear behaviour of single bolted T-stub connections", *Proc. of Connection in Steel Structures V*, Amsterdam, June, 53-64.

Gitlow, H.S., Levine, D.M. and Popovich, E.A. (2006), *Design for Six Sigma for Green Belts and Champions*, Prentice Hall Publishers, ISBN 0-13-185524-7, 1-720.

Guillot, J. (1987), "Threaded elements connection; Modeling and calculation", Ed. Engineering Techniques, Volume 1 B5560 to B5562, 75006, Paris, 1-56.

I-DEAS 11 NX (2004), UGS PLM Solutions Inc., I-DEAS Simulation Product Software, Release 11 ms4, 5800 Granite Parkway, Suite 600 Plano, Texas 75024, USA, http://www.ugs.com.

JMP (2005), The Statistical Discovery Software, Release 5.1, SAS Institute, Cary, NC, USA, http://www.jmp.com.

Junker, G.H. (1986), *Principle of Bolted Connections Calculation in Ultimate Service*, Technical Thesis. SPS-UNBARAKO S.A., Aulnay-sous-Bois.

Kishi, N., Ahmed, A., Yabuki, N. and Chen, W.F. (2001), "Nonlinear finite element analysis of top- and seat-angle with double web-angle connections", *Struct. Eng. Mech.*, **12**(2), 201-214.

Komuro, M., Kishi, N. and Chen, W.F. (2004), "Elasto-plastic FE analysis on moment-rotation relations of top- and seat-angle connections", *Proc. of Connection in Steel Structures V*, Amsterdam, June, 111-120.

Kowalske, D. (1973), *Berechnung exzentrisch belasteter Flanschverbindungen.* Ind. Anz. 9, (Ausgabe. Schrauben, Verbindungsel, Federn, Normt.), H. 1.
Kuehl, R.O. (1999), *Design of Experiments: Statistical Principles of Research Design and Analysis*, ISBN 0534368344, Duxbury Press, 2nd Edition, 1-688.
Lehnhoff, T.F., Ko, K.I. and McKay, M.L. (1994), "Member stiffness and contact pressure distribution of bolted joints", *J. Mech. Design*, ASME, **113**, 432-437.
Martinez-Martinez, M. (2002), *Study of Threaded Assemblies Behaviour: Calculation of Thread Stripping*, PhD Thesis, N° 653, INSA of Toulouse France.
Marty, D. (1994), *Study of Bolted Flanged Connection Subjected to Fatigue Loading,* Mechanical Engineering Master, INSA of Toulouse, France.
Montgomery, D.C. (2000), *Design and Analysis of Experiments*, Wiley 5th Edition, ISBN 0471316490, 1-672.
NF E27-009 norm (1979), *Fasteners – Fatigue Test Under Axial Load*, AFNOR Publications, 1st Edition, October, 1-10.
Oden, J.T. and Pires, E.B. (1983), "Non local and nonlinear friction laws and variational principles for contact problems in elasticity", *J. Appl. Mech.*, **50**, 67-76.
Rasmussen, J., Norgaard, I.B., Haastrup, O. and Haastrup, J. (1978), "A two body contact problem with friction", *Proc. of Euromech Colloquium*, NR 110 Rimforsa, 115-120.
Razavi, H. (2004), *Kinematic Hardening Cyclic Plasticity based Semi Meshless Finite Element Algorithms for Contact and Bolted Problems*, PhD Thesis, UMI Number 3145832, University of Texas at Arlington.
Rockey, K.C., Evans, H.R., Griffiths, D.W. and Nethercot, D.A. (1983), *The Finite Element Method. A Basic Introduction for Engineers*, Granada, London, J Wiley & Sons, New-York, ISBN 0-246-12053-3; 0-470-27459-X.
Sherbourne, A.N. and Bahaari, M.R. (1997), "Finite element prediction of end-plate bolted connection behaviour. I: Parametric study", *J. Struct. Eng.*, **123**(2), 157-164.
Taguchi, G. (1978), "Performance analysis design", *Int. J. Production Res.*, **16**(6), 521-530.
Taguchi, G. (1987), *The System of Experimental Design: Engineering Methods to Optimize Quality and Minimize Costs*, Quality Resources Publishers, ISBN 0527916218, 1-1176.
Taguchi, G. (2001), "Taguchi methods in LSI fabrication process", *Statistical Methodology, IEEE Int. Workshop, 6th.*, 1-6.
Tsai, H.C. and Kelly, J.M. (2005), "Buckling of short beams with warping effect included", *Int. J. Solids Struct.*, **42**, 239-253.
Vadean, A., Leray, D. and Guillot, J. (2006), "Bolted joints for very large diameter bearings - Numerical model development", *Finite Elem. Anal. Des.*, **42**(4), 298-313.
VDI 2230 BLATT 1 (2003), *Systematische Berechnung Hochbeanspruchter Schraubenver-bindungen Zylindrische Einschraubenverbindungen*, VDI Richtlinien, ICS 21.060.10, VDI-Gesellschaft Entwicklung Konstruktion Vertrieb, Fachberuch Konstruktion, Ausschuss Schraubenverbindungen.
Zaharia, R. and Dubina, D. (2006), "Stiffness of joints in bolted connected cold-formed steel trusses", *J. Constr. Steel Res.*, **62**, 240-249.

Appendix: Stiffness matrices of T-stub model elements and the force-displacement relationship

The developed model consists of bi-nodal beam and axial spring elements. Each node has three degree of freedom (u, v, θ).

Beam elements:

For a beam element ($i-j$), (Fig. 11), the force-displacement relationship is

$$\{F_{ij}\} = [K_{ij}]\{U_{ij}\} \tag{A.1}$$

where $\{F_{ij}\}$ and $\{U_{ij}\}$ are force and displacement vectors and $[K_{ij}]$ is the stiffness matrix of the beam element

in the local coordinates system (u, v, z). The expressions used are

$$\{F_{ij}\} = \{X_i \;\; Y_i \;\; M_i \;\; X_j \;\; Y_j \;\; M_j\}^T \text{ and } \{U_{ij}\} = \{u_i \;\; v_i \;\; \theta_i \;\; u_j \;\; v_j \;\; \theta_j\}^T \tag{A.2}$$

$$[K_{ij}] = \begin{bmatrix} \frac{ES}{l} & 0 & 0 & -\frac{ES}{l} & 0 & 0 \\ & \frac{12EI}{l^3} & \frac{6EI}{l^2} & 0 & -\frac{12EI}{l^3} & \frac{6EI}{l^2} \\ & & \frac{4EI}{l} & 0 & -\frac{6EI}{l^2} & \frac{2EI}{l} \\ & & & \frac{ES}{l} & 0 & 0 \\ & & & & \frac{12EI}{l^3} & -\frac{6EI}{l^2} \\ & & & & & \frac{4EI}{l} \end{bmatrix} \tag{A.3}$$

To change from the local to the global coordinates system, the transformation matrix $[T]$ is given by

$$[T] = \begin{bmatrix} \lambda & \mu & 0 & 0 & 0 & 0 \\ -\mu & \lambda & 0 & 0 & 0 & 0 \\ 0 & 0 & 1 & 0 & 0 & 0 \\ 0 & 0 & 0 & \lambda & \mu & 0 \\ 0 & 0 & 0 & -\mu & \lambda & 0 \\ 0 & 0 & 0 & 0 & 0 & 1 \end{bmatrix} \tag{A.4}$$

where $\lambda = \cos\varphi$ and $\mu = \sin\varphi$

Stiffness matrix $[\overline{K}_{ij}]$ of a beam element $(i-j)$ in the global coordinates system (x, y, z) is determined by

$$[\overline{K}_{ij}] = [T]^T[K_{ij}][T] \tag{A.5}$$

Properties of the beam elements modeling the bolted *T*-stub are resumed in Table 4.

For beam elements (part CA), dimensions b_{ij} and l_{ij} are mesh dependant. Stiffness matrix $[R_g]$ of the free structure is obtained by assembling the stiffness matrices of all the beam elements.

Table 4 Properties of beam elements of the model

Beam elements	Figs.	E	I	S	l	φ
Beam elements (part CA)	2 and 3	E_P	$\frac{b_{ij}h_p^3}{12}$	$b_{ij}h_p$	l_{ij}	0
Beam elements B_1L_1 and B_2L_2	2	E_P	$\frac{\pi(D_p^4 - D_t^4)}{64}$	A_P	$\frac{h_p}{2}$	$\frac{\pi}{2}$
Beam elements (bolts B_1E_1 and B_2E_2)	2 and 4	E_b	I_{bi}	A_{bi}	$\frac{h_b}{2}$	$-\frac{\pi}{2}$

Spring elements:
Stiffness matrix of the spring element, formulated in its local coordinate system, is given by

$$[K_{ij}] = \begin{bmatrix} k_{ij} & -k_{ij} \\ -k_{ij} & k_{ij} \end{bmatrix} \tag{A.6}$$

Axial stiffness k_{ij} depends on the spring $(i-j)$ position. it is considered equal to zero at the detachment location in the contact zone. Overall contact stiffness matrix $[R_c]$ of the structure is obtained by assembling the spring elements stiffness matrices.

Finally, global stiffness matrix $[R_T]$ is obtained by assembling matrices $[R_g]$ and $[R_c]$. The force-displacement relationship of the whole structure is expressed as in Algorithm 1, with the necessary boundary conditions.